

Magnetized accretion-ejection structures

V. Effects of entropy generation inside the disc

F. Casse and J. Ferreira

Laboratoire d'Astrophysique de l'Observatoire de Grenoble, B.P.53, 38041 Grenoble cedex 9, France

Received 28 April 2000 / Accepted 26 July 2000

Abstract. In this paper, steady-state MHD calculations of non-relativistic magnetized accretion discs driving jets are presented. For the first time, an energy equation describing the effects of entropy generation along streamlines is included. Using a simplified approach, we showed that thermal effects have a tremendous influence on the disc capability to feed jets with mass.

The disc ejection efficiency is measured by the parameter $\xi = d \ln \dot{M}_a / d \ln r$, where $\dot{M}_a(r)$ is the local disc accretion rate. While previous self-similar solutions were only able to produce jets with $\xi \sim 0.01$, solutions with a coronal heating display huge efficiencies up to $\xi \sim 0.5$. Moreover, taking thermal effects into account allows one to obtain both fast and slow magnetic rotators.

Since most of the jet properties (like asymptotic velocity or degree of collimation) depend on the mass load, it arises from this study that any quantitative result requires a detailed analysis of the disc energetics.

Key words: accretion, accretion disks – Magnetohydrodynamics (MHD) – stars: formation – ISM: jets and outflows – galaxies: nuclei – galaxies: jets

1. Introduction

1.1. Jets and discs

Astrophysical jets are observed in a wide variety of objects, from young protostars surrounded by a circumstellar accretion disc to compact objects in either close binary systems or active galactic nuclei. In all these systems, several observational evidences point towards strong links between accretion and ejection phenomena (Hartigan et al. 1995, Mirabel et al. 1998 and Serjeant et al. 1998). Thus, theorists must provide models where accretion and ejection can be simultaneously explained in a self-consistent way. More precisely, these models must provide a clear picture not only of how a fraction of the disc matter becomes an ejected flow, but also of the energetics involved (e.g., the ratio of the jet kinetic power to the accretion power). Indeed, some problematic objects show powerful jets produced from discs showing a

much lower activity than expected (Rutten et al. 1992, Di Matteo et al. 2000). We will call this the energy problem.

It is well known that the “standard” accretion disc model of Shakura & Sunyaev (1973) cannot explain jets. In this model, all the mass is accreted towards the central object while the liberated mechanical power (called accretion power) is radiated at its surfaces. However, it has been recognized that, under certain circumstances, the disc could become geometrically thick, hence allowing for an efficient advection of the thermal energy (Abramowicz et al. 1988). This has an important observational consequence. Indeed, these advection-dominated accretion flow (ADAF) models allow a sizeable fraction of the accretion power to be actually advected onto the central object. Thus, such a power would be observationally “lost” if this object happens to be a black hole. Moreover, it has been argued that such ADAFs might be hot enough to provide a launching mechanism for jets (Narayan & Yi 1995). As a consequence, one might have jets with a high kinetic power arising from low-luminosity discs. All this reasoning is fine, but no comprehensive work has been done showing such a possibility. There is however an alternative to this energy problem.

1.2. Models of magnetized discs driving jets

First, we recall that a very efficient launching mechanism is the presence of a large scale bipolar magnetic field threading the accretion disc (for an alternative view, see Lery et al. 1999). This magnetic field can be generated by a dynamo effect (see Rekowski et al. 2000) and/or by advection of an interstellar magnetic field (Mouschovias 1976). Indeed, since the seminal work of Blandford & Payne (1982), it has been showed that, combined with the disc rotation, such a field could (1) extract the disc angular momentum, (2) provide an acceleration force to a fraction of the mass and (3) maintain the jets self-collimated by a hoop-stress. Thus, explaining collimated jets would require one to revisit the standard model by self-consistently incorporating magnetic fields. We call these objects magnetized accretion-ejection structures (MAES).

The first attempt to describe such objects was made by Königl (1989), followed by Wardle & Königl (1993) and Li (1995, 1996). However, these works had two drawbacks. First, they did not self-consistently treat the disc vertical equilibrium,

thereby obtaining huge parameter spaces and, second, the overall energy budget was not considered.

A complete description of MAES has been presented in a series of papers where, thanks to a self-similar ansatz, all dynamical terms were included in the magnetohydrodynamic (MHD) equations (Ferreira & Pelletier 1993, 1995, Ferreira 1997, Casse & Ferreira 2000). In particular, it has been shown that a necessary condition for jet production is the reversal of the sign of the magnetic torque at the disc surface: while negative at the disc midplane (angular momentum extraction), it must become positive at the surface in order to magnetically propell matter. This condition provides a strong constraint on the properties of the MHD turbulence believed to exist inside discs. Casse & Ferreira (2000) provided a comprehensive scan of the parameter space of “cold” MAES, i.e. where enthalpy plays no role in jet dynamics. They assumed adiabatic magnetic surfaces and showed that, depending on the MHD turbulence properties, two kinds of “cold” MAES could exist:

- (1) discs where the magnetic torque due to the jets is much larger than the local “viscous” torque (of turbulent origin). These MAES are called “non-dissipative”. Indeed, almost all the available power feeds the jets and only a tiny fraction is locally dissipated and radiated by the disc (see also Ferreira & Pelletier 1993 and Ferreira 1997). Another important consequence of the larger magnetic torque is a disc density that is smaller than in a standard disc (for the same accretion rate). A non-dissipative MAES could then be optically thin, and is thus expected to provide a spectrum very much comparable to that of an ADAF.
- (2) discs where the magnetic torque is comparable to the viscous torque, called “dissipative” MAES. Such structures dissipate as radiation a power comparable to that carried away by the jets. No solution has been found with a dominant viscous torque.

Thus, MAES quite straightforwardly address the energy problem mentioned earlier. Instead of advecting energy onto the central object, as ADAF does, MAES put a sizeable fraction of the accretion energy into jets. In fact, everything depends on the properties of the MHD turbulence inside the disc, which are still unknown.

1.3. The “cold jet” approximation

Nonetheless, all these results (as well as all previous works on disc winds) rely on what happens to be a very important assumption, namely the “cold jet” approximation. Usually, in the literature, a “cold jet” is a jet where enthalpy plays no role in its launching (i.e., is negligible in the Bernoulli equation). Thus, in order to get ejection from the disc surface, the opening angle, defined as the angle between the poloidal magnetic field and the vertical axis, must be bigger than 30° (Blandford & Payne 1982). However, the crucial question is the amount of mass that can be loaded in the jet. This is **never** addressed in any steady-state numerical simulation, since the underlying accretion disc is merely a boundary condition. This mass load critically depends

on the force balance at the disc surface, where matter can still cross the magnetic field lines. In this transition layer from a resistive disc to an ideal MHD jet, the only force allowing matter to go up is the plasma pressure gradient (Ferreira & Pelletier 1995). Thus, the vertical profile of the temperature does play a role in the launching process. Since it mainly occurs in the resistive MHD region, a negligible enthalpy in the ideal MHD zone does not mean that it had no influence on jet formation.

In this paper, we will show that the precise treatment of the energy equation must be done correctly, especially at the disc surface. This is a *sine qua non* condition in order to get realistic quantitative answers concerning the capability of accretion discs to launch jets. In particular, the presence of a hot corona could drastically change the whole picture. Because cooling and heating processes depend on density and temperature, the conditions at the disc surface vary with the radius and depend also on the astrophysical context studied (e.g. around a compact object or a young star). Here, our purpose is just to illustrate this stinging but crucial point by using some crude prescription. We will investigate specific astrophysical contexts in forthcoming papers.

In Sect. 2, we recall the basic stationary MHD equations describing a MAES and define the relevant disc and jet parameters. Sect. 3 is the cornerstone of this paper. We introduce the local disc energy equation with the assumption we used and discuss the constraints imposed by the global energy conservation. Thermal effects on stationary jet production are then analyzed. In Sect. 4, we show some typical self-similar MAES solutions and describe two extreme cases. We finally conclude in Sect. 5.

2. Magnetized accretion-ejection structures

2.1. Basic MHD stationary equations

Thanks to axisymmetry, the vectorial quantities expressed in cylindrical coordinates (r, ϕ, z) , can be decomposed into poloidal and toroidal components, e.g. $\mathbf{u} = \mathbf{u}_p + \Omega r \mathbf{e}_\phi$ and $\mathbf{B} = \mathbf{B}_p + B_\phi \mathbf{e}_\phi$. A bipolar configuration allows us to describe the poloidal magnetic field as

$$\mathbf{B}_p = \frac{1}{r} \nabla a \times \mathbf{e}_\phi, \quad (1)$$

where $a(r, z)$ is an even function of z and $a = \text{constant}$ describes a surface of constant magnetic flux ($a = r A_\phi$, A_ϕ being the toroidal component of the potential vector). The following set of equations describes a steady-state, non-relativistic MAES,

- Mass conservation

$$\nabla \cdot \rho \mathbf{u} = 0 \quad (2)$$

- Momentum conservation

$$\rho \mathbf{u} \cdot \nabla \mathbf{u} = -\nabla P - \rho \nabla \Phi_G + \mathbf{J} \times \mathbf{B} + \nabla \cdot \mathbf{T} \quad (3)$$

- Ohm’s law and toroidal field induction

$$\eta_m J_\phi \mathbf{e}_\phi = \mathbf{u}_p \times \mathbf{B}_p \quad (4)$$

$$\nabla \cdot \left(\frac{\nu'_m}{r^2} \nabla r B_\phi \right) = \nabla \cdot \frac{1}{r} (B_\phi \mathbf{u}_p - \mathbf{B}_p \Omega r) \quad (5)$$

where ρ is the density of matter, P the thermal pressure, $\Phi_G = -GM_*/(r^2+z^2)^{1/2}$ the gravitational potential, $\mathbf{J} = \nabla \times \mathbf{B}/\mu_o$ the current, \mathbf{T} the “viscous” stress tensor, $\nu_m = \eta_m/\mu_o$ and ν'_m the (anomalous) poloidal and toroidal magnetic diffusivities. All transport coefficients appearing in the above set of equations, namely ν_m , ν'_m and ν_v (“viscosity”, contained in \mathbf{T}), are assumed to be of turbulent origin. The state equation used is the perfect gas law

$$P = nk_B T \quad (6)$$

where k_B is the Boltzmann constant, $n = \rho/m_p$ (m_p being the proton mass) and T the plasma temperature.

The last equation is the energy equation. Until now, it has been replaced by a simple prescription on the temperature, namely isothermal or adiabatic magnetic surfaces (see e.g. Ferreira & Pelletier 1995 for a discussion on this subject). The aim of the present paper is to study the thermal effects on jet production. Therefore, we must consider the energy equation, which can be written as

$$\rho T \frac{dS}{dt} = \rho T \mathbf{u}_p \cdot \nabla S = Q \quad (7)$$

where S is the specific entropy and Q is the local source of entropy, arising from the difference between heating and cooling processes (see Sect. 3 for more details).

2.2. Dynamical parameters of MAES

The set of equations (2) to (7) completely describes a steady-state, non-relativistic MAES. We recall here the definitions of the parameters used:

- The disc aspect ratio

$$\varepsilon = \frac{h(r)}{r} \quad (8)$$

- The MHD turbulence level (measuring the strength of the poloidal magnetic diffusivity at the disc midplane)

$$\alpha_m = \left. \frac{\nu_m}{V_A h} \right|_{z=0} \quad (9)$$

- The magnetic Prandtl number (measuring the strength of the turbulent viscosity)

$$\mathcal{P}_m = \left. \frac{\nu_v}{\nu_m} \right|_{z=0} \quad (10)$$

- The magnetic diffusivity anisotropy

$$\chi_m = \left. \frac{\nu_m}{\nu'_m} \right|_{z=0} \quad (11)$$

where $h(r)$ is the vertical disc scale height and V_A the Alfvén speed at the disc midplane. These four parameters are defined locally and could, in principle, vary along the disc. In our study however, they are assumed constant. Also, while the disc aspect ratio ε remains free (because we did not treat the real energy equation), the three other turbulence parameters must remain

free, until the development of a full theory of MHD turbulence. All other disc and jet quantities can be expressed in terms of these parameters (see Casse & Ferreira 2000, hereafter CF). As an example, the usual alpha coefficient of Shakura & Sunyaev is given by

$$\alpha_v = \left. \frac{\nu_v}{C_s h} \right|_{z=0} = \mathcal{P}_m \alpha_m^* \quad (12)$$

where $\alpha_m^* = \nu_m/C_s h = \alpha_m(\mu/\gamma)^{1/2}$, $\mu = (V_A/\Omega_K h)^2$ is a measure of the magnetic field strength (Ω_K is the Keplerian rotation rate) and γ the adiabatic index. Note that, since steady state MAES require fields close to equipartition (i.e. $\mu \leq 1$, Ferreira & Pelletier 1995), one has $\alpha_m^* < \alpha_m$.

2.3. Generalized ideal MHD integrals

Inside the disc, accreting matter must cross the field lines. Thus, a stationary configuration requires turbulent magnetic diffusivities. This turbulence is believed to be triggered inside the disc by some MHD instability, but decays vertically on (say) a disc scale height. In the ideal MHD regime characterizing the jets, integrals of motion appear in the basic MHD equations. These are

$$\mathbf{u}_p = \frac{\eta(a)}{\mu_o \rho} \mathbf{B}_p \quad (13)$$

$$\Omega_*(a) = \Omega - \eta \frac{B_\phi}{\mu_o \rho r} \quad (14)$$

$$\Omega_* r_A^2 = \Omega r^2 - \frac{r B_\phi}{\eta} \quad (15)$$

where $\eta(a) = \sqrt{\mu_o \rho_A}$ is a constant along a magnetic surface and ρ_A is the density at the Alfvén point, where the poloidal velocity u_p reaches the poloidal Alfvén velocity $V_{A,p}$. The rotation rate of a magnetic surface is $\Omega_*(a)$ and r_A is the Alfvén radius. Following Blandford & Payne (1982), we introduce the following jet parameters

$$\begin{aligned} \lambda &= \frac{\Omega_* r_A^2}{\Omega_o r_o^2} \\ \kappa &= \eta \frac{\Omega_o r_o}{B_o} \\ \omega_A &= \frac{\Omega_* r_A}{V_{A,p,A}}. \end{aligned} \quad (16)$$

The subscript “o” refers to quantities evaluated at the disc midplane, “A” at the Alfvén surface. These parameters are directly related to the disc parameters (see CF). The last ideal MHD invariant is the Bernoulli integral. This invariant is modified by the presence of heating, contrary to the three former invariants. By projecting the momentum conservation on a magnetic surface and using thermodynamics relations, one gets (Chan & Henriksen 1980, Sauty & Tsinganos 1994)

$$E(a) = \frac{u^2}{2} + \frac{\gamma}{\gamma-1} \frac{P}{\rho} + \Phi_G - \Omega_* \frac{r B_\phi}{\eta} - \mathcal{H}(s, a) \quad (17)$$

where the enthalpy (second term) will be hereafter represented by H and

$$\mathcal{H}(s, a) = \int_{s^+}^s \frac{Q(s', a)}{\rho(s', a)u_p(s', a)} ds' \quad (18)$$

is a heating term that depends on the curvilinear coordinate s along a given magnetic surface (labelled by a constant $a(r, z)$). Here, s^+ represents the coordinate of the transition between the resistive and the ideal MHD regimes (above the disc surface). Jets from quasi-Keplerian accretion discs are energetically possible if

$$E(a) = \Omega_o^2 r_o^2 \left(\lambda - \frac{3}{2} + \frac{\gamma}{\gamma - 1} \frac{T^+}{T_o} \varepsilon^2 \right). \quad (19)$$

is positive at the base of the jet. Thus, either the magnetic lever arm λ is larger than $3/2$ or some heating occurred in the underlying resistive layers. This last possibility arises whenever the disc is already hot (i.e. thick $\varepsilon \sim 1$ or slim $\varepsilon < 0.3$ discs) and/or if some coronal heating leads to an increase of the temperature T^+ at the disc surface.

3. Entropy generation in MAES

3.1. Local entropy generation

The local energy equation (7) is

$$\begin{aligned} Q &= \rho T \frac{dS}{dt} = \rho \frac{dH}{dt} - \frac{dP}{dt} \\ &= \frac{\gamma}{\gamma - 1} \frac{k_B}{m_p} \rho \mathbf{u}_p \cdot \nabla T - \mathbf{u}_p \cdot \nabla P. \end{aligned} \quad (20)$$

In a thin (or slim) accretion disc, the gradient of any plasma quantity is mostly vertical. So the main influence of an entropy source Q occurs whenever the plasma velocity becomes vertical namely, at the disc surface. There, a non-vanishing Q will have two distinct and important consequences. First, it raises the plasma temperature (T^+) and second, it causes an increase of the vertical plasma pressure gradient. The vertical component of the momentum conservation becomes

$$\rho u_z \frac{\partial u_z}{\partial z} \simeq - \frac{\partial P}{\partial z} - \rho \Omega_K^2 z - \frac{\partial}{\partial z} \frac{B_\phi^2 + B_r^2}{2\mu_o}. \quad (21)$$

In this equation, the only force that can gently expell matter from the disc is the vertical plasma pressure gradient. Thus, increasing this gradient through an entropy source Q allows new configurations to exist. For example, with parameters (ε , α_m , \mathcal{P}_m , χ_m) similar to those of a ‘‘cold’’ MAES (i.e. $Q \simeq 0$), a solution with an entropy source would display a larger vertical force, allowing thereby a larger mass flux κ . Or, with the same entropy source, one could get a steady ejection from a MAES with a larger magnetic pinching, corresponding to turbulence parameters impossible to achieve with $Q \simeq 0$.

Thus, we see that both the amplitude and the vertical profile of the entropy source Q are important features for stationary MAES. In fact, there is a local entropy source Q only if there

is a slight discrepancy between the local heating and cooling terms, namely

$$Q = (\Gamma_{eff} + \Gamma_{turb} + \Gamma_{ext}) - (\Lambda_{rad} + \Lambda_{turb}) \quad (22)$$

where

$$\Gamma_{eff} = \eta_m J_\phi^2 + \eta'_m J_p^2 + \eta_v |r \nabla \Omega|^2 \quad (23)$$

is the effective Joule and viscous heating, Γ_{turb} is a turbulent heating term which cannot be described by simple anomalous transport coefficients (e.g., the term Γ_{eff}), Γ_{ext} is an external source of energy (typically due to some illumination by UV or X-rays, hence maximum at the disc surface),

$$\Lambda_{rad} = \nabla \cdot \mathbf{S}_{rad} \quad (24)$$

is the radiative cooling (\mathbf{S}_{rad} being the radiative flux) and Λ_{turb} is a cooling due to a turbulent energy transport, which is most probably also taking place inside turbulent discs (see e.g. Shakura et al. 1978).

If the disc is optically thick, the radiative flux \mathbf{S}_{rad} can be written in a simple way using the diffusion approximation (e.g. Ferreira & Pelletier 1993). However, both the amplitude and the vertical profile of the turbulent energy transport Λ_{turb} are unknown. This is really problematic, since this term could be the leading cooling term (like convection, see Ferreira & Pelletier 1995). On the other hand, magnetized discs may well have active coronae, hence a non negligible Γ_{turb} mainly acting at the disc surface (Galeev et al. 1979, Heyvaerts & Priest 1989, Miller & Stone 2000). Therefore, even if we neglect any external influence, the only term whose amplitude and vertical profile are really known is Γ_{eff} . Thus, following Narayan & Yi (1995) for ADAFs, we define a parameter f as

$$f = \frac{\int_V Q dV}{\int_V \Gamma_{eff} dV} = \frac{\int_V Q dV}{P_{diss}} \quad (25)$$

where the integral is made over the volume V occupied by the disc and P_{diss} is the total power which could be dissipated inside the disc. With this prescription, the amplitude of the entropy source Q is controlled by f , but not its vertical profile. This profile depends on the relative importance of the various terms appearing in Eq. (22) and, as such, is beyond our actual knowledge. To tackle this difficult problem, we will assume the profile and discuss the corresponding physical implications on jet production.

3.2. Global energy conservation

A strong constraint on this parameter f arises from the global energy conservation. If we integrate the local energy conservation equation over the whole volume V , we get the following energy budget

$$P_{acc} + P_{ext} = 2P_{jet} + 2P_{rad} \quad (26)$$

where P_{acc} is the power liberated through the accretion process,

$$P_{ext} = \int_V \Gamma_{ext} dV \quad (27)$$

is the total input of energy due to an external source, P_{jet} is the total power (mechanical, magnetic and thermal) carried away by one jet (hence leaving the disc at its surface) and P_{rad} the luminosity radiated at one surface (see Appendix A).

In this paper, we do not consider any external source of energy, thus $P_{ext} = 0$. Moreover, we do not expect in a quasi-Keplerian flow the accreted turbulent energy to be significant with respect to the mechanical energy. Thus, we assume that the total turbulent power is negligible, namely

$$P_{turb} = \int_V (\Gamma_{turb} - \Lambda_{turb}) dV = 0. \quad (28)$$

The characteristic power, liberated by a MAES located around a central mass M_* , between the radii r_i and r_e and fed with an accretion rate $\dot{M}_{ae} = \dot{M}_a(r_e)$, is

$$P_{lib} \equiv \eta_{lib} \frac{GM_* \dot{M}_{ae}}{2r_i} \quad (29)$$

where the efficiency η_{lib} is given in Appendix B. In discs producing jets, the accretion rate is a function of the radius. We therefore define the local ejection efficiency as

$$\xi = \frac{d \ln \dot{M}_a}{d \ln r}. \quad (30)$$

In terms of the fiducial value P_{lib} , the global energy conservation (26) of thin (or even slim) MAES is (see Appendix B for details)

$$\frac{P_{acc}}{P_{lib}} = (1 - \xi) \left(1 + \frac{1}{2} \frac{\varepsilon \Lambda}{1 + \Lambda} \right) \quad (31)$$

providing jets powered with

$$\frac{2P_{jet}}{P_{lib}} = \frac{\Lambda}{1 + \Lambda} \left| \frac{B_\phi^+}{qB_o} \right| + \frac{2\gamma}{\gamma - 1} \frac{T^+}{T_o} \xi \varepsilon^2 - \xi \quad (32)$$

and a disc luminosity of

$$\frac{2P_{rad}}{P_{lib}} = (1 - f) \frac{P_{diss}}{P_{lib}} = \frac{P_{acc} - 2P_{jet}}{P_{lib}} \quad (33)$$

Here, the parameter Λ is the ratio of the magnetic torque to the viscous torque at the disc midplane and q is a measure of the radial current density at the disc midplane (see CF for more details).

From the above energy budget, it becomes obvious that two extreme cases can be accounted for, namely

- $f \ll 1$: cooling and heating processes balance each other very effectively at every point, so that there is no entropy generation at all ($Q \simeq 0$). In this case, the dissipated power P_{diss} is finally radiated at the disc surfaces.
- $f = 1$: a large entropy source is generated in this case, because of a turbulent transport more efficient than radiative cooling and the presence of another heating process (e.g. coronal heating). As a consequence, no power is radiated at all, the accretion power being transferred into the jets.

The case $f > 1$ can still be obtained but requires an extra source of energy (P_{ext} or P_{turb}). This is also true when $f < 1$ but the disc luminosity exceeds that provided by Eq. (33).

3.3. Constraints on steady-state jet production

The trans-Alfvénic condition is modified by the possible presence of a heating term along the flow. This can be directly seen in the function g , defined as $\Omega = \Omega_*(1 - g)$ and evaluated at the Alfvén surface

$$g_A^2 = 1 - \frac{3}{\lambda} - \frac{1}{\omega_A^2} + \frac{2}{\lambda^{3/2}(1 + z_A^2/r_A^2)^{1/2}} + \frac{2}{\lambda} \left[\frac{\gamma}{\gamma - 1} \frac{T^+ - T_A}{T_o} \varepsilon^2 + \frac{\mathcal{H}(s_A, a)}{\Omega_o^2 r_o^2} \right] \quad (34)$$

The subscripts “o” and “A” denote a quantity measured, respectively, at the disc midplane and at the Alfvén surface. A necessary condition for trans-Alfvénic cold jets is usually expressed as

$$\omega_A^2 > 1, \quad (35)$$

implying these jets are fast rotators (Michel 1969, Pelletier & Pudritz 1992, Ferreira 1997). However, this condition is only strictly valid for very large magnetic lever arms ($\lambda \rightarrow \infty$). The generalized trans-Alfvénic condition is in fact

$$g_A^2 > 0 \quad (36)$$

Thus, Eq. (34) shows that entropy generation inside the disc (leading to a large T^+) or alternatively, some coronal heating (significant $\mathcal{H}(s_A, a)$), allows the fulfillment of the above condition with $\omega_A < 1$. Therefore, we expect slow rotators to emerge as (magneto-)thermally driven jets.

Following the same reasoning as Ferreira (1997) in Sect. 3, but considering the generalized Bernoulli equation, we obtain an inequality constraining the magnetic lever arm

$$\frac{\lambda}{\lambda - 1} < \lambda - 3 + \frac{2}{\lambda^{1/2}(1 + z_A^2/r_A^2)^{1/2}} + \frac{2\gamma}{\gamma - 1} \frac{T^+}{T_o} \varepsilon^2 + 2 \frac{\mathcal{H}(s_A, a)}{\Omega_o^2 r_o^2}. \quad (37)$$

This quite complex relation is equivalent to $\lambda > \lambda_{min} = 1 + \zeta$. This shows that, to produce super-Alfvénic jets, there must be a minimum magnetic lever arm λ_{min} . Thus, steady-state MAES cannot display an ejection efficiency larger than

$$\xi_{max} = \frac{1}{2\zeta} \frac{\Lambda}{1 + \Lambda} \quad (38)$$

The exact value of ζ is strongly dependent on Q (both amplitude f and vertical profile). Basically, the more heat is added, the more mass is ejected. For example, for $T^+ \leq T_o$, $\zeta = 3$ while for $T^+ \simeq \varepsilon^{-2} T_o$, $\zeta \simeq 0.3$. Thus, as already pointed out, the major constraints on ξ arise from the disc vertical equilibrium in the resistive MHD regime and the energy balance.

4. Numerical results

4.1. The self-similar ansatz

In this section, we briefly describe the radial self-similarity that enables us to consider both the resistive, viscous disc and the

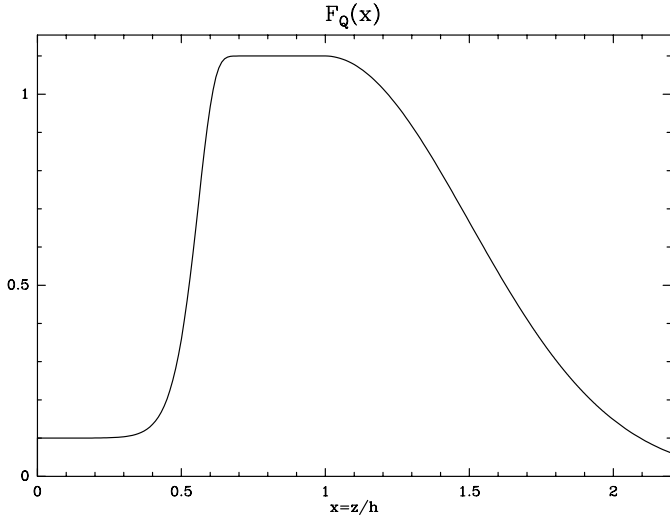


Fig. 1. Vertical profile of the entropy generation function Q for a given ejection index $\xi = 0.1$. The value of this function at the disc midplane ($x = 0$) is imposed by the self-similar radial scalings (see text). The integral of this function is measured by the parameter f . The particular shape shown here (increasing towards the disc surface) mimics a coronal heating.

ideal MHD jet, including an exact treatment of all dynamical terms. Any physical quantity $A(r, z)$ is written as

$$A(r, z) = A_e \left(\frac{r}{r_e} \right)^{\alpha_A} F_A(x) \quad (39)$$

where $x = z/h(r)$ and r_e is the outer radius of the magnetized disc. This special ansatz allows to separate the variables so that the full MHD equations become a set of non-ordinary (they contain three singularities) differential equations. The values of the radial exponents (given in Ferreira & Pelletier 1993) are all linked to the ejection index ξ . For example, the magnetic flux becomes

$$a(r, z) = a_e \left(\frac{r}{r_e} \right)^{\beta} F_a(x) \quad (40)$$

with $\beta = 3/4 + \xi/2$. Inside this framework, the entropy source Q must be written as

$$Q = Q_e \left(\frac{r}{r_e} \right)^{\xi-4} F_Q(x) \quad (41)$$

where, using Eq. (20), its value at the disc midplane must satisfy

$$\begin{aligned} Q_o &= Q(r, z = 0) = \left(\frac{\gamma}{\gamma - 1} + \alpha_P \right) \frac{P_o u_{po}}{r} \\ &= \left(\frac{\gamma}{\gamma - 1} + \xi - \frac{5}{2} \right) \frac{P_o u_{po}}{r}. \end{aligned} \quad (42)$$

This is a very strong constraint which also occurs in self-similar ADAF models. There $\xi = 0$, so an ADAF must have $\gamma \neq 5/3$ in order to get some advected heating at the disc midplane. Here, we choose an adiabatic index $\gamma = 5/3$ and scale the vertical profile $F_Q(x)$ with the parameter f . We display in Fig. 1

a typical profile corresponding to a discrepancy between cooling and heating processes, occurring mainly at the disc surface. We did however play with slightly different vertical profiles (see Fig. 8).

The set of MHD equations has three critical points in the ideal MHD regime. These critical points are the slow-magnetosonic, the Alfvén and the fast-magnetosonic points. The solutions presented here share the same behavior obtained in previous studies (Ferreira 1997, CF). The magnetized flow passes through the slow and Alfvén points (the regularity conditions impose the values of μ and ξ) and then encounters the fast-magnetosonic point in a recollimation motion. None of these solutions pass through the last critical point (see Vlahakis et al. 2000).

4.2. From magnetically-driven to thermally-driven jets

As showed in Sect 3.1, the entropy generation increases the plasma pressure gradient, thereby allowing an enhanced vertical mass flux. In particular, jets are now possible in configurations where the magnetic pinching force would be overwhelming and squeeze the disc. Thus, thermal effects significantly enlarge the parameter space of MAES ($\varepsilon, \alpha_m, \mathcal{P}_m, \chi_m$).

In order to illustrate such an effect (strong magnetic compression balanced by entropy generation), we choose a MAES configuration described by the following parameters: $\varepsilon = 0.1$, $\alpha_m = 1.5$ ($\alpha_m^* = 0.8$), $\mathcal{P}_m = 1$, $\chi_m = 1.5$. The chosen disc aspect ratio is relevant in the astrophysical systems we consider (see Appendix C). Fig. 2 shows relevant quantities obtained with the same vertical profile F_Q (see Fig. 1) and increasing values for f .

First, a minimum heating ($f \sim 0.001$) is here required otherwise the thermal plasma gradient cannot counteract the magnetic pinching force. Note that this minimum heating decreases with decreasing α_m (because of the weaker toroidal magnetic compression). Second, as expected, both the mass flux κ and coronal temperature T^+ grow as f increases. Their maximum values depend on the chosen set of disc parameters. In a consistent way, the magnetic lever arm λ diminishes with f . Third, as f increases, thermal effects become significant and there is a transition between “cold” and “hot” outflows. Indeed, when f is very small, the jets show the usual characteristics of a “cold” outflow, namely a fast magnetic rotator ($\omega_A > 1$), a large magnetic lever arm λ , a small mass load κ and a coronal temperature T^+ smaller than that in the disc. At the opposite extreme, when f is close to unity, the jets are slow magnetic rotators ($\omega_A < 1$), have small magnetic lever arms, high mass loads and high coronal temperatures.

We will label as “hot” those jets whose initial enthalpy plays a significant role in their launching. We display in Figs. 3 and 4, the Bernoulli constants $E(a)$ and their different components, for the two extreme jets obtained in Fig. 2 (respectively $f = 0.82$ and $f = 0.002$). In the “hot” jet, the enthalpy at the base is of the same order as the MHD Poynting flux. The jet acceleration in the sub-Alfvénic region is mostly due to the decrease in the enthalpy. This shows the importance of thermal effects, although

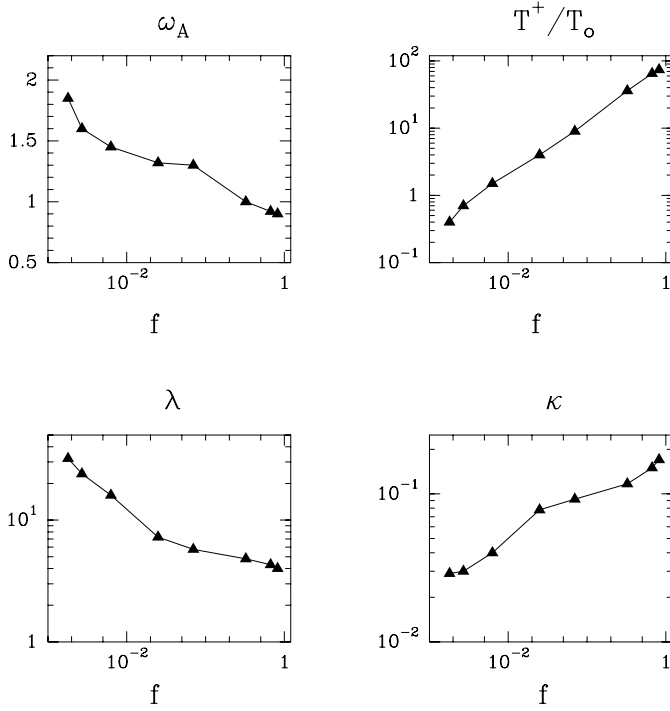


Fig. 2. Variation of several quantities with the entropy parameter f for a given magnetic configuration: $\varepsilon = 0.1$, $\alpha_m = 1.5$ ($\alpha_m^* = 0.8$), $\mathcal{P}_m = 1$, $\chi_m = 1.5$. Non-relativistic jets from Keplerian accretion discs can be either fast rotators ($\omega_A > 1$) or slow rotators ($\omega_A < 1$), depending on the amplitude of f . The coronal temperature increases monotonously with f . The plots in mass load κ and magnetic lever arm λ illustrate the fact that the more entropy generated, the more mass is loaded (see Sect. 3.1).

the Blandford & Payne criterion (opening angle larger than 30°) is, here, still verified. In the “cold” jet however, the enthalpy is negligible and the acceleration is due to the decrease of the poloidal current.

In order to clearly distinguish “cold” (magnetically-driven) from “hot” (thermally-driven) jets, we look at the decrease along the jet of the poloidal current, defined as

$$I = \frac{2\pi}{\mu_o} r B_\phi. \quad (43)$$

Indeed, this current is a measure of the transfer of MHD Poynting flux into kinetic energy flux (see Ferreira 1997). We plot in Fig. 5 the ratio I_A/I_{SM} of the current still available at the Alfvén point to the current provided at the base of the flow (at the slow-magnetosonic point). For small f (here $f < 0.1$), this ratio remains high because a tiny fraction of mass has been loaded in the jet. As f increases, this ratio decreases because the enhanced mass load requires more magnetic energy to be used. But at some point ($f > 0.1$), the thermal energy reservoir supplants the MHD Poynting flux in propelling matter until the Alfvén point. Thus, the ratio is now increasing because of this new energy supply. The two regimes shown in Fig. 5 define a “cold jet” and a “hot jet” zone.

For a given MAES, there is always an upper limit to the entropy generation (besides the overall energy conservation con-

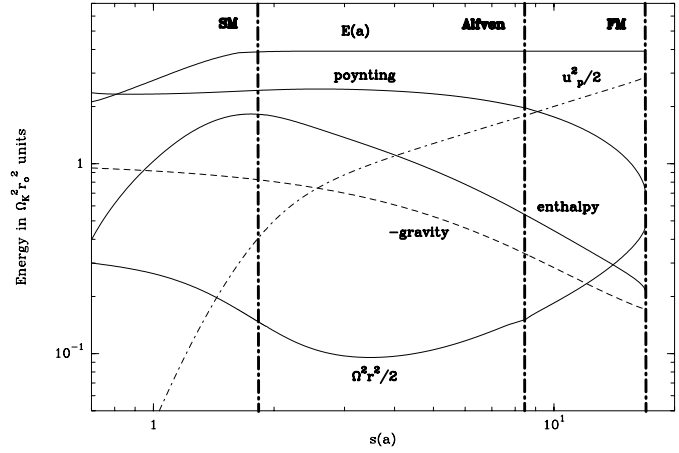


Fig. 3. Bernoulli invariant $E(a)$ and its components along a given magnetic surface ($s(a) = z(a)/h_o$), for the hottest jet ($f = 0.82$) in Fig. 2. The quantities are normalized to the square of the angular velocity at the footpoint of the magnetic surface ($\Omega_o^2 r_o^2$). Enthalpy is of the same order as the MHD Poynting flux in the corona, the signature of a “hot” jet.

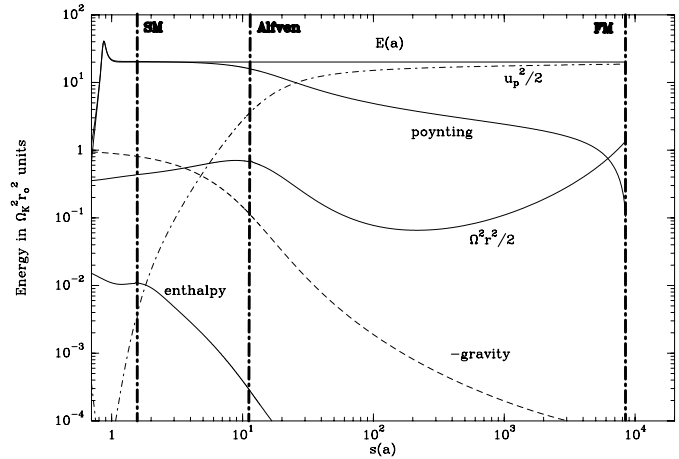


Fig. 4. Same plot as in Fig. 3, but for the coldest jet ($f = 0.002$) of Fig. 2. The enthalpy does not play any role in the jet energetics. This is the signature of a “cold” jet.

straint) coming from the requirement that g_A must always remain smaller than unity (i.e. B_ϕ remains negative). Indeed, the available current at the Alfvén point is given by

$$\frac{I_A}{I_{SM}} = g_A \frac{\lambda}{\lambda - 1}. \quad (44)$$

The increase of this ratio for increasing f is mainly due to the increase of g_A (see Fig. 2). Thus, there is a maximum f allowed (which can be smaller than unity) for steady-state MAES.

A transition from “cold” to “hot” jets requires the crossing of a zone where a large mass load (provided by the enhanced plasma pressure gradient) is still accelerated. This is only achieved if a sufficient amount of toroidal magnetic field is present (B_ϕ is the most relevant ingredient of the Poynting flux) and/or if the thermal energy reservoir is sufficient. However, depending on the magnetic configuration, the jet mass load

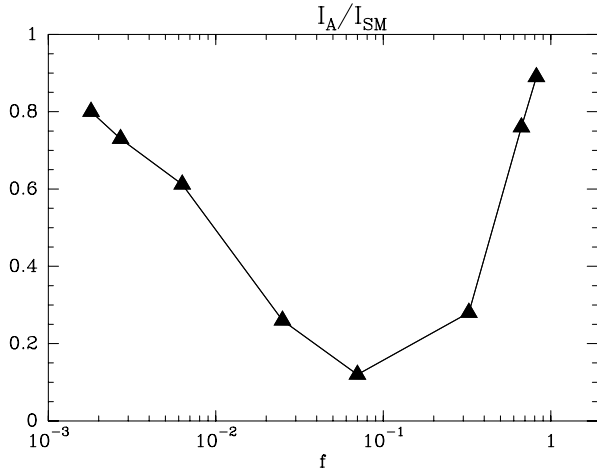


Fig. 5. Ratio I_A/I_{SM} of the current at the Alfvén point to the current at the slow-magnetosonic point as a function of the entropy parameter f , for the same MAES as in Fig. 2. As f increases, there is a transition from one regime to the other. The first regime corresponds to “cold” jets, where the thermal energy is insignificant and the mass load is small. The second regime corresponds to “hot” jets, where a large thermal energy supplants the Poynting flux in propelling matter in the sub-Alfvénic region.

could increase with f faster than the enthalpy. As a result, configurations with a weak toroidal magnetic field would not be able to steadily launch jets in a zone where the enthalpy is not sufficient. As an example, we provide in Figs. 6 and 7 a magnetic configuration with a smaller turbulence level ($\alpha_m = 1.2$), hence a toroidal magnetic field smaller than in the previous case. This time, no solution was found between $0.02 < f < 0.5$.

4.3. Two extreme MAES

Because of the extreme sensibility of the mass load κ to the entropy source Q , we will not give a parameter space including these thermal effects. Indeed, both the amplitude f and the vertical profile F_Q should be obtained by the resolution of a realistic energy equation including cooling and heating terms. These terms (especially the cooling function) depend critically on the astrophysical context studied. Our purpose here is to show the broad range of available solutions by providing two extreme MAES configurations.

4.3.1. A dense, slow “hot” jet

In this extreme solution, a huge ($f = 1$) entropy generation occurs above the disc surface, see pannel e) in Fig. 8. This might be achieved with some sort of non-local coronal heating, efficiently transporting upwards the thermal energy released in the underlying layers of the disc.

For this pedagogical example, we choose a magnetic configuration described by the following disc parameters: $\varepsilon = 0.1$, $\alpha_m = 4$ ($\alpha_m^* = 1.8$), $\mathcal{P}_m = 1$, $\chi_m = 1.4$. It exhibits straight poloidal magnetic field lines inside the disc and a factor $q = 1.012$, leading to a torque ratio $\Lambda = 2.6$ (comparable mag-

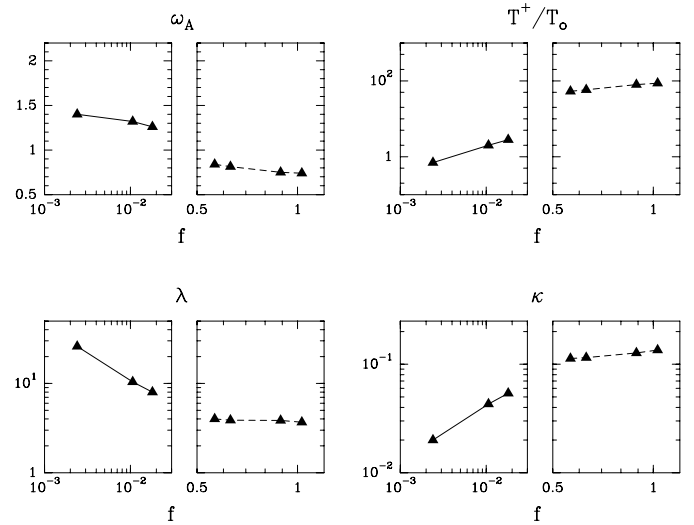


Fig. 6. Same plots as in Fig. 2, but for a weaker turbulence level $\alpha_m = 1.2$. The two jet regimes are now split. “Cold” jets exist only for $f < 0.02$, “hot” jets only for a large entropy generation, $f > 0.5$.

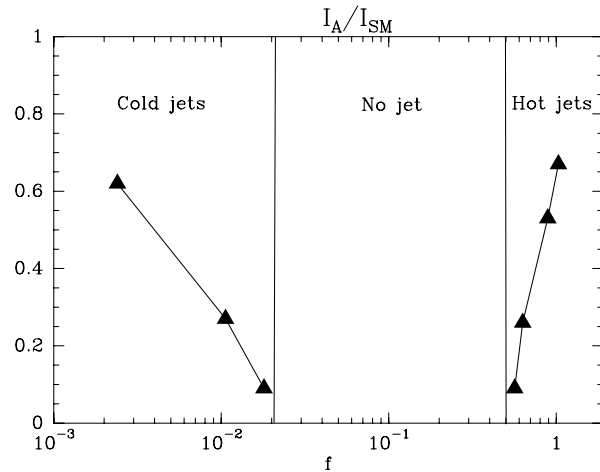


Fig. 7. Same plot as in Fig. 5, but for a MAES with a weaker turbulence level $\alpha_m = 1.2$. A forbidden zone appears where both the MHD Poynting flux and the thermal energy are too small to propel the mass loaded.

netic and viscous torques). The required magnetic field must be quite small, $\mu = 0.26$ (ie. a plasma beta of 7.7 at the disc midplane).

The enormous release of thermal energy allowed a very large ejection, namely $\xi = 0.456$. The corresponding jet parameters are a mass load $\kappa = 1.04$, a magnetic lever arm $\lambda = 1.9$ and a rotator parameter $\omega_A = 1.65$. Although this solution is “hot”, it is still a fast rotator. This is because the toroidal field at the disc surface is high, $|B_\phi^+| = 0.94B_o$, despite straight poloidal field lines (large α_m , see CF).

The disc corona is hot and quite dense and the jet does not widen much before recollimation occurs (see Fig. 8). This widening is, however, sufficient to produce jets where most of the available energy has been transferred into poloidal kinetic energy, namely

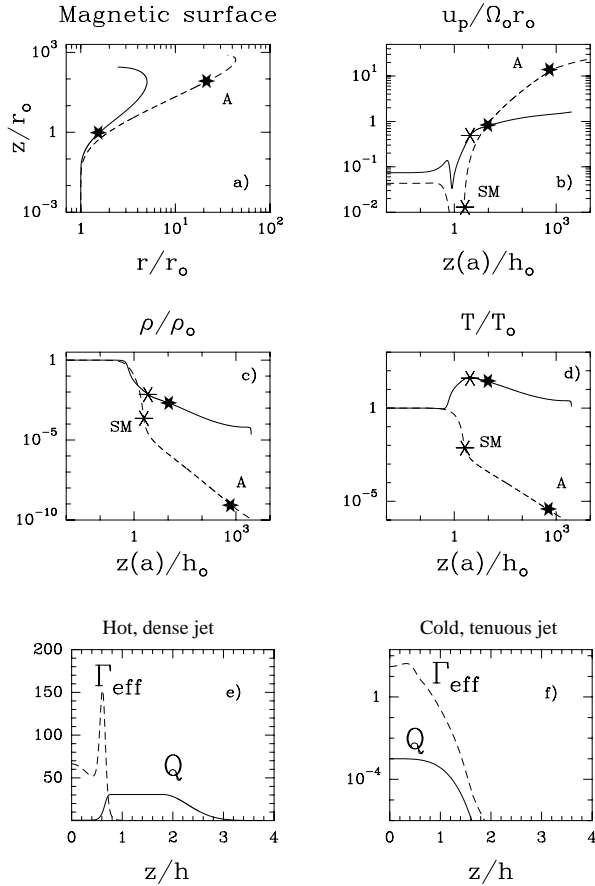


Fig. 8. Plots of various characteristics of the two extreme (“hot” and “cold”) jets presented in Sect. 4.3: **a** poloidal cross-section of the magnetic surfaces anchored at a radius r_o ; **b** poloidal velocity of the plasma along a magnetic surface in units of the Keplerian speed at its footpoint; **c** and **d**, plasma density and temperature along a magnetic surface normalized to their values at the disc midplane. The “hot”, dense jet is drawn in solid line while the “cold”, tenuous jet is in dashed line. The cross symbolizes the locus of the slow-magnetosonic (SM) point and the star the locus of the Alfvén (A) point. Panels **e** and **f** show the effective (viscous and Ohmic) heating term Γ_{eff} and the prescribed entropy source Q at a constant radius, normalized to the same quantity.

$$u_{p\infty} \simeq \sqrt{2E(a)} \quad (45)$$

along every magnetic surface. The presence of a large thermal energy allows a terminal velocity larger than $\Omega_o r_o \sqrt{2\lambda - 3}$, which is the characteristic value obtained in “cold” flows ($\Omega_o r_o$ is roughly the Keplerian speed at the footpoint r_o of the magnetic surface). Fig. 9 shows a cross section of such a solution, settled around a compact object (upper image). Even in this extremely “hot” solution, the jet opening angle at the transition between resistive and ideal MHD regimes is $\theta^+ = 37^\circ$, thus still fulfilling the Blandford & Payne condition for “cold” jets.

The global energy budget is here exceedingly simple. Since $f = 1$, all the accretion power is finally converted into jet kinetic power, $P_{acc} = 2P_{jet} \simeq 0.58 P_{lib}$. Again, we do not claim this is a realistic solution, but we want to point at the extreme sensibility of the produced jets to the disc energetics.

4.3.2. A tenuous, fast “cold” jet

Here, we show an example of a jet launched from a MAES with an almost negligible entropy generation, namely $f = 5 \cdot 10^{-5}$ see panel **f** in Fig. 8. This slight discrepancy between heating and cooling processes occurs only inside the disc. Thus, this solution requires no energy source above the disc, neither a coronal heating nor an illumination.

The MAES is described by the following disc parameters: $\varepsilon = 0.1$, $\alpha_m = 0.3$ ($\alpha_m^* = 0.2$), $\mathcal{P}_m = 1$, $\chi_m = 0.047$. It exhibits a very strong curvature of the poloidal magnetic field lines inside the disc and a factor $q = 0.25$, leading to a torque ratio $\Lambda = 15.67$ (dominant magnetic torque at the disc mid-plane). Here, the required magnetic field is closer to equipartition, $\mu = 0.745$ (ie. a plasma beta of 2.7 at the disc midplane).

In this case, the strong compression due to the vertical magnetic pressure gradient almost forbids the formation of a jet. The presence of a slight entropy generation however allows an ejection with an efficiency $\xi = 0.001$. The corresponding jet parameters are a tiny mass load $\kappa = 2.8 \cdot 10^{-4}$, a huge magnetic lever arm $\lambda = 440$ and a rotator parameter $\omega_A = 1.2$. Again, this is not a “very” fast rotator despite the small mass load, because of the small value of the toroidal field at the disc surface ($|B_\phi^+| = 0.12 B_o$).

The jet is “cold”, with a very strong adiabatic cooling due to its large widening (see Fig. 8). This widening resulted in a very efficient acceleration of the ejected plasma, leading to an asymptotic poloidal velocity ~ 23 times the Keplerian speed at the field lines footpoint. This is because of the huge magnetic lever arm λ . In particular, relativistic speeds could be expected if such a MAES is settled in the vicinity of a compact object. Indeed, if we define σ_∞ as the asymptotic ratio of the MHD Poynting flux to the kinetic energy flux, one gets an asymptotic Lorentz factor of

$$\gamma_\infty = 1 + \frac{2\lambda - 3}{12(1 + \sigma_\infty)} \left(\frac{3r_g}{r_o} \right), \quad (46)$$

where $r_g = 2GM_*/c^2$ is the Schwarzschild radius of the central object. Of course, a full calculation of the relativistic MHD equations should be performed in order to get the value of σ_∞ . As an example, if some equipartition is achieved ($\sigma_\infty = 1$, Li et al. 1992), one could, in principle, get jets with asymptotic Lorentz factors ranging from ~ 36 ($r_o \sim 3r_g$) to ~ 4 ($r_o \sim 30r_g$).

Fig. 9 shows a cross section of such a solution, settled around a compact object (lower image). The opening angle θ^+ is quite large, 53° , typical of a “cold” outflow. The global energy budget is here more subtle than in the previous case. Indeed, we obtain an accretion power of $P_{acc} \simeq 1.09 P_{lib}$, jets fed with a total power of only $2P_{jet} \simeq 0.45 P_{lib}$ with the remaining power being radiated at the disc surfaces, namely $2P_{rad} \simeq 0.64 P_{lib}$. Thus, we do have a dissipative MAES producing “cold” jets. The very strong curvature of the poloidal magnetic field lines yields a strong toroidal current, hence a large Ohmic dissipation. Moreover, the large anisotropy of the MHD turbulence ($\chi_m = 0.047$), provides also a large dissipation of the toroidal magnetic field (see Eq. (23)). Hence, the dissipated power P_{diss} , which

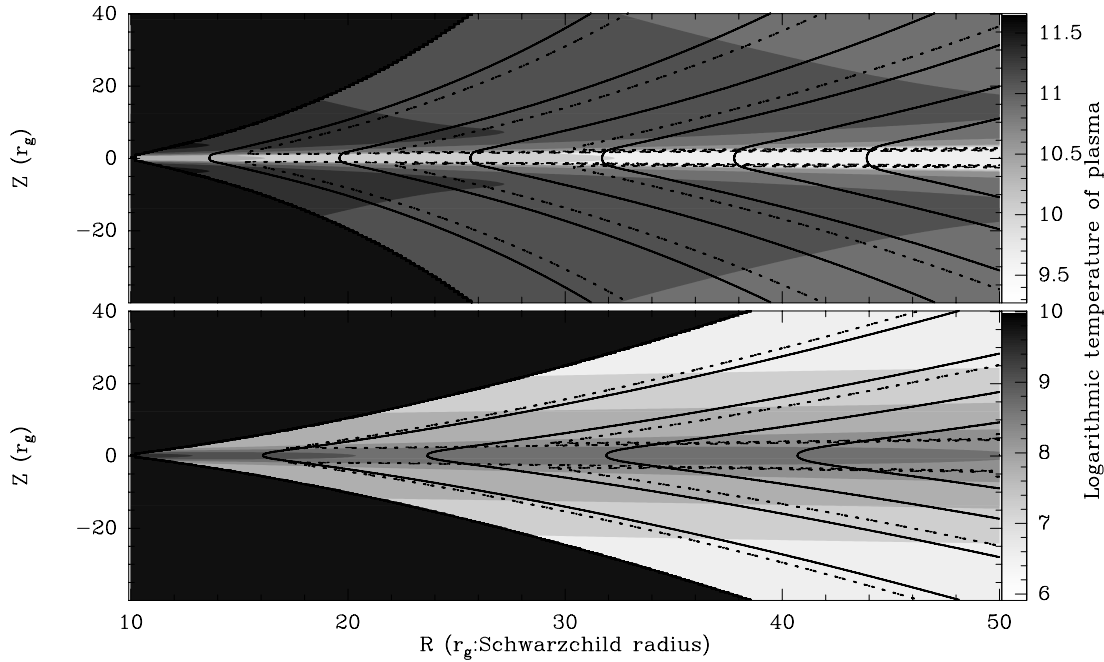


Fig. 9. Cross-sections of two extreme magnetized accretion-ejection structures (MAES), settled around a neutron star of $M_* = 1.4M_\odot$ and fed with an accretion rate of $\dot{M}_{ae} = 10^{-12} M_\odot/\text{yr}$. The poloidal magnetic field is shown in solid lines, streamlines are dashed and the grey contours represent the logarithm of the plasma temperature. Both MAES have the same temperature at the disc midplane. The upper image is an extremely “hot” MAES ($f = 1$) with an entropy source located above the disc surface. This solution has a huge ejection efficiency of $\xi = 0.456$, plasma reaching an asymptotic velocity 1.6 times the Keplerian speed $\Omega_o r_o$ at the magnetic field lines footprint r_o . The lower image is a “cold” MAES ($f = 5 \cdot 10^{-5}$) with no heating source above the disc. Such a solution has $\xi = 0.001$ with asymptotic velocities 23 times $\Omega_o r_o$.

is here converted into radiation, is quite large. Eq. (32) shows that the exact amount of energy powering the jets depends on the ratio $|B_\phi^+ / qB_o|$. Here this ratio is equal to 0.48, namely a generated toroidal magnetic field at the disc surface half the expected value (measured by q). This decrease of the toroidal magnetic field is due to this enhanced magnetic diffusivity ν'_m .

5. Conclusion

In this paper, we removed a basic assumption of most theoretical works dealing with axisymmetric, stationary Keplerian discs launching jets (MAES). Indeed, the disc energy equation is usually neglected, using either adiabatic (Casse & Ferreira 2000) or isothermal (Wardle & Königl 1993, Li 1995, 1996, Ferreira 1997) magnetic surfaces.

We used a self-similar ansatz allowing us to take into account all dynamical terms in the resistive, viscous disc as well as in the ideal MHD jet. The transition between the accretion and the ejection motions is self-consistently described. We modelled the entropy increase along each streamline by prescribing the vertical profile of the heat effectively converted into entropy. This is an approach very similar to that used in ADAF models, with a significant distinction. Indeed, in the case of MAES, the main part of the heat released in the disc could be absorbed by the jet instead of being advected onto the central object.

The ability to steadily produce jets lies in the rather subtle disc vertical equilibrium. Both gravity and the chosen bipolar magnetic topology vertically pinch the accretion disc. Thus,

mass can only be lifted from the disc by the plasma pressure gradient. Because a local entropy generation enhances this gradient (see Eq. (20)), the amount of mass escaping the disc can be much larger. Alternatively, tiny mass loads, impossible to achieve in previous MAES calculations, are now reachable. Indeed, a huge magnetic compression can be now balanced by some amount of heating. Moreover, there is a second important consequence of entropy generation, namely enthalpy generation. This enthalpy is carried away by the outflowing material and can be converted afterwards into kinetic energy. To summarize, entropy generation results in dynamical (measured by the ejection index ξ) and thermal (measured by the coronal temperature T^+) effects. For the first time, this is self-consistently illustrated in a global energy budget of MAES. This paper has illustrated that heating is as important in steady jet formation from an accretion disc as in steady outflow release around embedded sources (e.g. Lery et al. 1999).

We are now in a position to provide clear diagnostics on steady-state MHD simulations of jets from Keplerian accretion discs. Indeed, all effects acting on the ejection process itself are taken into account. Of course, this study was done under the self-similar assumption, but the links between MHD invariants are local and, as such, independent of this ansatz. Besides, in a quasi-Keplerian disc where gravity (which is self-similar) is the dominant driving term, we expect self-similar solutions to be quite reasonable. For example, local jet parameters (mass load κ , magnetic lever arm λ and rotator parameter ω_A) as well as

the shape of the Alfvén surface (ie. conical), are comparable to stationary solutions obtained with full 2D, time-dependent numerical simulations of “cold” jets (Krasnopolsky et al. 1999).

Ustyugova et al. (1999), using another MHD code and starting with a split-monopole poloidal magnetic field, obtained a non-conical Alfvén surface. However, their local jet parameters remain comparable to those obtained in this study. Indeed, they have larger mass loads and smaller magnetic lever arms, but with a prescribed temperature satisfying $C_s^+/\Omega_{Kor} = (T^+/T_o)^{1/2}\varepsilon \geq 0.3$. Because the authors assumed a flat disc (no flaring at all, hence $\varepsilon \ll 1$), this boundary condition requires a coronal temperature larger than the temperature at the disc midplane. As a consequence, a significant entropy generation must take place in the underlying accretion disc.

Ouyed & Pudritz (1997) also obtained stationary jets from Keplerian discs with full 2D, time-dependent MHD simulations. They assumed power-law magnetic fields for their boundary conditions at the jet basis and “cold” adiabatic magnetic surfaces. Surprisingly, they obtained jets with very large mass loads ($\kappa > 0.6$) and very small magnetic lever arms ($\lambda < 3.5$). This large mass flux is compatible with a large toroidal magnetic field at the jet basis (~ 1.5 times the vertical field). However, the disc vertical equilibrium cannot handle such a strong pinching in a non-dissipative disc ($f \ll 1$, see CF). Besides, we showed in Sect. 3.3 that thin discs with $T^+ \leq T_o$ require $\lambda > 4$, a value smaller than those obtained in these simulations. One possible way to reconcile our analytical result with their numerical simulation is to realize that the jet basis used in all MHD simulations of that kind is **not** the disc surface but some surface above it. In particular, it could be located above a region where a coronal heating (allowing a large mass load κ) was followed by a very strong cooling (negligible enthalpy at the “jet basis”). One must then be very cautious when identifying boundary conditions as being the disc surface. Indeed, the real issue of jet formation is the mass load provided by the underlying accretion disc.

The effects of entropy generation, theoretically shown in this paper, were numerically confirmed by the self-similar solutions. For example, the surplus of thermal energy, obtained with a significant parameter f , allowed jets that would be labelled as slow magnetic rotators ($\omega_A < 1$). We did not intent to explore any parameter space because of the extreme sensitivity of the mass load κ to the entropy source Q (both vertical profile and amplitude, measured by f). For example, a very weak entropy generation triggered inside the disc could give birth to very tenuous, fast jets while a huge entropy generation just above the disc surface could make dense, slow jets.

Without exploring the parameter space, we nevertheless obtained a much wider range of MAES parameters than under an adiabatic assumption (CF), namely mass loads $10^{-4} \leq \kappa \leq 1$ (ie. $0.001 \leq \xi < 0.5$), magnetic lever arms $1.9 \leq \lambda \leq 440$ and magnetic rotator parameters $0.7 < \omega_A < 2.2$. Such huge ejection efficiencies could have a strong impact on disc spectral energy distributions. Indeed, if the disc is optically thick, the effective temperature can be written (Ferreira & Pelletier 1995)

$$T_{eff} \propto r^{-\frac{3}{4} + \frac{\xi}{4}}. \quad (47)$$

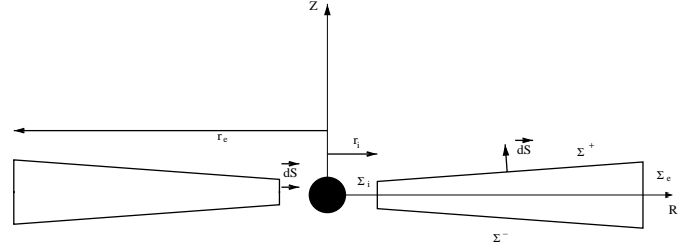


Fig. A.1. Cross-section of the volume V occupied by the disc and the corresponding bounding surfaces (lateral Σ_i and Σ_e , upper Σ^+ and lower Σ^-). The upper and lower surfaces correspond to the location of a vanishing radial velocity (typically at $z^+ \sim h(r)$).

Thus MAES with large ejection efficiencies would display a flat distribution (possibly up to $T_{eff} \propto r^{-1/2}$). However, only a precise treatment of the plasma energetics (including all heating, cooling and transport processes) provides the exact value of the disc ejection efficiency ξ . This can only be done for a given astrophysical context, since all these energetic processes (and possibly MHD turbulence α_m , \mathcal{P}_m and χ_m) strongly depend on the plasma properties. Therefore, any quantitative modelling of a MAES must include a complete treatment of the energy equation.

Acknowledgements. The authors would like to thank Guy Pelletier and Jean Heyvaerts for useful comments and fruitful discussions.

Appendix A: global energy conservation

The local energy conservation equation can be written as

$$\nabla \cdot (\rho \mathbf{u}_p \left(\frac{u^2}{2} + \Phi_G + H \right) + \mathbf{S}_{MHD} - \mathbf{u} \cdot \mathbf{T}) = \rho T \mathbf{u}_p \cdot \nabla S - \Gamma_{eff}. \quad (A.1)$$

where \mathbf{S}_{MHD} is the MHD Poynting flux, \mathbf{T} the turbulent stress tensor, H the enthalpy, S the specific entropy and Γ_{eff} the effective Ohmic and viscous heating (see Sect. 3.1). The second law of thermodynamics (22),

$$\rho T \mathbf{u}_p \cdot \nabla S = \Gamma_{eff} + (\Gamma_{turb} - \Lambda_{turb}) + \Gamma_{ext} - \nabla \cdot \mathbf{S}_{rad} \quad (A.2)$$

is then incorporated into Eq. (A.1). To get the global energy conservation, we integrate this equation on the whole volume V occupied by the disc (Ferreira 1994, Henriksen 1996). We thus define Σ^+ and Σ^- as the disc surfaces and Σ_i (Σ_e) the lateral surfaces at $r = r_i$ ($r = r_e$, see Fig. A.1). The disc surface is here precisely defined at the locus where the radial velocity vanishes, namely where $u_r(r, z^+ = x^+ h(r)) = 0$.

After integration, we get

$$P_{acc} + P_{ext} + P_{turb} = 2P_{jet} + 2P_{rad} \quad (A.3)$$

where the accretion power P_{acc} is the power liberated by the accretion flow (the difference between what comes in at r_e and goes out at r_i), $P_{ext} = \int_V \Gamma_{ext} dV$ is the power provided by an external source, $P_{turb} = \int_V (\Gamma_{turb} - \Lambda_{turb}) dV$ is a source

of turbulent energy, P_{jet} is the power carried by the outflowing matter and $P_{rad} = \int_{\Sigma^\pm} \mathbf{S}_{rad} \cdot d\mathbf{S}$ is the luminosity emitted at the disc surfaces.

The available turbulent power P_{turb} comes from the small scale turbulent motions, but is carried along by the laminar accretion flow. Therefore, there is also a flux of specific turbulent energy \mathcal{E}_{turb} crossing the inner and outer sides of the disc, which implies

$$P_{turb} = - \int_{\Sigma_i} \rho \mathbf{u}_p \mathcal{E}_{turb} \cdot d\mathbf{S} - \int_{\Sigma_e} \rho \mathbf{u}_p \mathcal{E}_{turb} \cdot d\mathbf{S} \quad (\text{A.4})$$

We redefine the accretion power P_{acc} by including P_{turb} inside. The total accretion power is then

$$P_{acc} = - \int_{\Sigma_i} [\rho \mathbf{u}_p \mathcal{E} + \mathbf{S}_{MHD} + \mathbf{S}_{rad} - \mathbf{u} \cdot \mathbb{T}] \cdot d\mathbf{S} - \int_{\Sigma_e} [\rho \mathbf{u}_p \mathcal{E} + \mathbf{S}_{MHD} + \mathbf{S}_{rad} - \mathbf{u} \cdot \mathbb{T}] \cdot d\mathbf{S} \quad (\text{A.5})$$

where the expression of the MHD Poynting flux in the resistive regime is given in Ferreira & Pelletier (1993) and

$$\mathcal{E} = \frac{u^2}{2} + \Phi_G + H + \mathcal{E}_{turb} \quad (\text{A.6})$$

is the advected specific energy of the flow (laminar and turbulent). The jet power is given by

$$P_{jet} = \int_{\Sigma^\pm} [\mathbf{S}_{MHD} + \rho \mathbf{u}_p \mathcal{E}] \cdot d\mathbf{S} = \int_{\Sigma^\pm} \rho \mathbf{u}_p E(a) \cdot d\mathbf{S} \quad (\text{A.7})$$

where $E(a)$ is the Bernoulli invariant (17) since, at the disc surface, the flow is in ideal MHD regime. Finally, we obtain

$$P_{acc} + P_{ext} = 2P_{jet} + 2P_{rad} \quad (\text{A.8})$$

which is the global energy conservation equation of a MAES.

Appendix B: self-similar energy conservation

In the self-similar framework used here, the global energy conservation can be expressed in terms of the fiducial power

$$P_{lib} = \eta_{lib} \frac{GM_* \dot{M}_{ae}}{2r_i} \quad \text{where} \quad \eta_{lib} = \frac{\left(\frac{r_i}{r_e}\right)^\xi - \left(\frac{r_i}{r_e}\right)}{1 - \xi} \quad (\text{B.1})$$

and local disc parameters. The accretion power is a sum of various terms, namely $P_{acc} = P_{acc}^{mec} + P_{acc}^{th} + P_{acc}^{MHD} + P_{acc}^{rad} + P_{acc}^{vis} + P_{turb}$. The mechanical contribution to P_{acc} is

$$\frac{P_{acc}^{mec}}{P_{lib}} \simeq (1 - \xi)(2 - \delta^2 - m_s^2 \varepsilon^2) \quad (\text{B.2})$$

$\delta = \Omega_o/\Omega_K$ (Ω_K is the Keplerian rotation rate) and $m_s = u_{po}/\Omega_K h_o$ being defined in CF. The advection of enthalpy by the accreting material decreases the liberated energy by a factor

$$\frac{P_{acc}^{th}}{P_{lib}} \simeq -2(1 - \xi) \frac{\gamma}{\gamma - 1} \varepsilon^2 \quad (\text{B.3})$$

while the MHD Poynting flux gives a positive contribution

$$\frac{P_{acc}^{MHD}}{P_{lib}} \simeq \frac{1 - \xi}{2} \frac{\Lambda}{1 + \Lambda} \left| \frac{B_\phi^+}{qB_o} \right| \tan \theta^+ \delta^2 \varepsilon \quad (\text{B.4})$$

where θ^+ is the angle between the magnetic field lines and the vertical axis at the disc surface ($x = x^+$). The presence of a turbulent viscosity produces a radial angular momentum flux through the disc, hence a flux of energy. This contribution to P_{acc} is

$$P_{acc}^{vis} = - \frac{P_{lib}}{1 + \Lambda} \frac{3\delta^2}{2\eta_{lib}} \frac{r_i}{r_e} - \int_{\Sigma_i} (\mathbf{u} \cdot \mathbb{T}) \cdot d\mathbf{S} \quad (\text{B.5})$$

where the second term is evaluated at the inner edge of the disc. There, it is usually assumed that the viscous torque is equal to zero, $\mathbb{T}(r_i) = 0$, leaving only a loss of energy at the disc outer edge.

Finally, the total power carried by the jets is

$$\begin{aligned} \frac{2P_{jet}}{P_{lib}} &= \frac{\Lambda}{1 + \Lambda} \left| \frac{B_\phi^+}{qB_o} \right| (1 - \varepsilon x^+ \tan \theta^+) \delta^2 \\ &+ \frac{2\gamma}{\gamma - 1} \frac{T^+}{T_o} \xi \varepsilon^2 \\ &- \xi \left[\frac{2}{(1 + \varepsilon^2 x^+)^{1/2}} - \left(\frac{u^+}{\Omega_o r_o} \right)^2 \right] \end{aligned} \quad (\text{B.6})$$

where u is the total velocity of matter.

Appendix C: disc thickness

In this appendix, we focus on the calculation of the disc aspect ratio imposed by the energy transport. To illustrate the full range of possible astrophysical contexts, we first consider systems where the disc plasma is ‘‘cold’’, dense and slow (young stellar objects) then systems where the disc plasma is ‘‘hot’’, tenuous and fast (around compact objects).

It is useful to identify which heating process dominates. In the case of MAES, we are able to estimate the ratio of viscous heating to Ohmic heating at the disc midplane, namely

$$\left. \frac{\eta_v |r \nabla \Omega|^2}{\eta_m J_\phi} \right|_{z=0} = \frac{9}{4\mathcal{P}_m \mu (1 + \Lambda)^2 \varepsilon^2} \quad (\text{C.1})$$

and

$$\left. \frac{\eta_v |r \nabla \Omega|^2}{\eta'_m J_p^2} \right|_{z=0} = \frac{3\mu}{\varepsilon^2}. \quad (\text{C.2})$$

For thin ($\varepsilon \ll 1$) or even slim disc ($\varepsilon < 0.3$), we have $\mathcal{P}_m \sim 1$, $\mu \sim 1$, $\chi_m \leq 1$ and $\Lambda \leq \varepsilon^{-1}$. The viscous heating is always dominant for solutions with comparable torques ($\Lambda \sim 1$).

We have the same approach than in the standard model (Shakura & Sunyaev 1973) since the viscous heating is the dominant heating source (we neglect Ohmic heating) and since the disc is assumed to be optically thick. Although the energy transport processes are unknown, we can safely assume that the

fraction $(1-f)$ of heating is fully transported to the disc surface where it is radiated at the photosphere,

$$\sigma T_{eff}^4 = \int_0^h \eta_v \left(r \frac{d\Omega}{dr} \right)^2 dz. \quad (C.3)$$

The effective temperature T_{eff} is related to the central temperature via the optical depth of the disc ($T_{eff}^4 \sim T^4/\tau$). Because we have assumed that the total pressure gradient equals the plasma pressure gradient, there is a direct link between the central temperature T_o and the “photospheric” height of the disc.

We thus validate the assumption of thin discs in the inner regions and checked the assumption of an optically thick disc.

C.1. Young stellar objects

In this context, the opacity of the disc can be fitted by a Rosseland grain opacity such as $\kappa_R = 0.1T^{1/2} \text{ cm}^2 \cdot \text{g}^{-1}$ (see Bell & Lin 1994). We obtain

$$\varepsilon_{phot} \equiv \frac{h_{phot}}{r} = 0.07(1-f)^{1/9} \alpha_v^{-1/9} \left(\frac{\dot{M}_a}{10^{-7}M_\odot/yr} \right)^{2/9} \left(\frac{M_*}{M_\odot} \right)^{-1/3} \quad (C.4)$$

The resulting optical depth is

$$\begin{aligned} \tau &= \int_0^{h_{phot}} \rho \kappa_R dz \simeq \kappa_R \rho_o h_{phot} \\ &= \frac{0.925}{\alpha_v^{10/9} (1-f)^{1/9} (1+\Lambda)} \left(\frac{\dot{M}_a}{10^{-7}M_\odot/yr} \right) \\ &\quad \times \left(\frac{M_*}{M_\odot} \right)^{1/3} \left(\frac{r}{1AU} \right)^{-1} \end{aligned} \quad (C.5)$$

This disc is indeed optically thick if the parameter α_v and/or the torque ratio Λ are small ($\alpha_v \sim 10^{-2}$ in YSO).

C.2. Compact objects (AGN, microquasars)

In the inner region of such systems, the Thomson opacity dominates. We thus obtain

$$\varepsilon_{phot} = \frac{0.6}{\alpha_v^{1/10}} (1-f)^{1/10} \times \left(\frac{\dot{M}_a}{M_\odot/yr} \right)^{1/5} \left(\frac{M_*}{M_\odot} \right)^{-3/10} \left(\frac{r}{3r_g} \right)^{1/20} \quad (C.6)$$

where $r_g = 2GM_*/c^2$ is the Schwarzschild radius. If we take $M_* = 10^7 M_\odot$ and $\dot{M}_a = 1 M_\odot/yr$ as fiducial values for AGN, we get $\varepsilon_{phot} \simeq 3 \cdot 10^{-3} (1-f)^{1/10} \alpha_v^{-1/10}$.

In the case of microquasars, we assume $M_* = 10 M_\odot$ and $\dot{M}_a = 10^{-7} M_\odot/yr$, so we get $\varepsilon_{phot} \simeq 10^{-2} (1-f)^{1/10} \alpha_v^{-1/10}$.

The corresponding optical depth is

$$\tau = \frac{2.4 \cdot 10^8}{\alpha_v^{4/5} (1-f)^{1/5} (1+\Lambda)} \left(\frac{r}{3r_g} \right)^{-3/5}$$

$$\times \left(\frac{\dot{M}_a}{M_\odot/yr} \right)^{3/5} \left(\frac{M_*}{M_\odot} \right)^{-2/5}. \quad (C.7)$$

As long as the photospheric disc aspect ratio remains smaller than unity, these discs remain optically thick. We must keep in mind that the photospheric height given in this appendix is a lower limit since we have neglected other heating sources. Indeed we can see, by looking at Eqs. (C.1) and (C.2), that MAES dominated by the magnetic torque ($\Lambda \geq \varepsilon^{-1}$) can provide Ohmic heating larger (but of the same order) than viscous heating. We thus choose a disc aspect ratio larger than those calculated here, namely $\varepsilon = 0.1$ (a value at the intersection of thin and slim discs).

References

- Abramowicz M.A., Czerny B., Lasota J.P., Szuszkiewicz E., 1988, ApJ 332, 646
 Bell K.R., Lin D.N.C., 1994, ApJ 427, 987
 Blandford R.D., Payne D.G., 1982, MNRAS 199, 883
 Chan K.L., Henriksen R.N., 1980, ApJ 241, 534
 Casse F., Ferreira J., 2000, A&A 353, 1115 (CF)
 Di Matteo T., Quataert E., Allen S.W., Narayan R., Fabian A.C., 2000, MNRAS 311, 507
 Ferreira J., Pelletier G., 1993, A&A 276, 625
 Ferreira J., 1994, Ph.D. Thesis, Université Paris VII
 Ferreira J., 1997, A&A 319, 340
 Ferreira J., Pelletier G., 1995, A&A 295, 807
 Galeev A.A., Rosner R., Vaiana G.S., 1979, ApJ 229, 318
 Hartigan P., Edwards S., Ghandour L., 1995, ApJ 452, 736
 Henriksen R.N., 1996, In: Tsinganos K.C. (eds.) Solar and Astrophysical Magnetohydrodynamic Flows. Kluwer, Dordrecht
 Heyvaerts J., Priest E.R., 1989, A&A 216, 230
 Königl A., 1989, ApJ 342, 208
 Krasnopolsky R., Li Z.-Y., Blandford R., 1999, ApJ 526, 631
 Lery T., Henriksen R.N., Fiege J.D., 1999, A&A 350, 254
 Li Z.-Y., Chiueh T., Begelman M.C., 1992, ApJ 394, 459
 Li Z.-Y., 1995, ApJ 444, 848
 Li Z.-Y., 1996, ApJ 465, 855
 Michel F.C., 1969, ApJ 158, 727
 Miller K.A., Stone J.M., 2000, ApJ 534, 398
 Mirabel I.F., Dhawan V., Chaty S., et al., 1998, A&A 330, L9
 Mouschovias T.Ch., 1976, ApJ 206, 753
 Narayan R., Yi I., 1995, ApJ 444, 231
 Ouyed R., Pudritz R.E., 1997, ApJ 482, 712
 Pelletier G., Pudritz R.E., 1992, ApJ 394, 117
 Rekowski M.V., Rüdiger G., Elstner D., 2000, A&A 353, 813
 Rutten R.G.M., van Paradijs J., Tinbergen J., 1992, A&A 260, 213
 Sauty C., Tsinganos K., 1994, A&A 287, 893
 Serjeant S., Rawlings S., Lacy M., et al. 1998, MNRAS 294, 494
 Shakura N.I., Sunyaev R.A., 1973, A&A 24, 337
 Shakura N.I., Sunyaev R.A., Zilitinkevitch S.S., 1978, A&A 62, 179
 Ustyugova G.V., Koldoba A.V., Romanova M.M., Chetchetkin V.M., Lovelace R.V.E., 1999, ApJ 516, 221
 Vlahakis N., Tsinganos K., Sauty C., Trussoni E., 2000, to be published in MNRAS (astro-ph/0005582)
 Wardle M., Königl A., 1993, ApJ 410, 218